Available online at www.sciencedirect.com

ScienceDirect

Procedia Structural Integrity 24 (2019) 852–865

Structural Integrity Procedia

www.elsevier.com/locate/procedia

AIAS 2019 International Conference on Stress Analysis

An original FE modelling of a longitudinal multi-passes seam welding

Simone Trupiano[a*], Valerio G. Belardi[a], Pierluigi Fanelli[b], Francesco Vivio[a], Luca Gaetani[c]

[a] *Department of Enterprise Engineering, University of Rome Tor Vergata, Via del Politecnico, 1, 00133, Rome, Italy*
[b] *Department of Economics, Engineering, Society and Business Organization, University of Tuscia, Largo dell'Università, 01100, Viterbo, Italy*
[c] *Eleo2 Engineering S.r.l., Via Benedetto Stay, 69, 00143 Rome, Italy*

Abstract

Both finite element and analytical methods for simulation of welding are essential to predict residual stress and distortions of welded components. Best FE modelling is obtained by using solid elements for thermo-structural simulation with high computational cost. In this contest, an equivalent modelling of plates based on shell elements is proposed in order to streamline the simulations. The equivalent model is composed of n levels of shell elements, centered on the weld seam, in order to evaluate rotations and translations typical of a multi-pass weld. There are as many levels as the number of the weld passes that compose the seam. The interconnection between the n shell levels is realized by rigid beam elements. The latter ones are connected to shell elements by constraint equations.
Solid brick models of the plates are used as a benchmark for the equivalent models in thermal and mechanical simulations.
The equivalent modelling is in good agreement with solid results, showing a strong decrease of computational burden, enabling the simulation of large welded models in operative conditions.

Peer-review under responsibility of the AIAS2019 organizers

Keywords: Welding simulation; Shell elements; Residual stress; Welding distortion; Butt joint

* Corresponding author. Tel.: 0039-0672597143.
E-mail address: simone.trupiano@uniroma2.it

Peer-review under responsibility of the AIAS2019 organizers
10.1016/j.prostr.2020.02.075

1. Introduction

It is well known that weldments are essential in naval, automotive, Oil and Gas industries to joint plates, shells or pipes. In welding, base material is exposed to extreme temperature gradients, with high thermal expansion and microstructural changes in the Heat Altered Zone. These severe conditions bring about distortions and residual stress in the welded zone. During the welding process distortions hinder the good control of welding parameters and cause final misalignments in the created joint. In the last two decades, several analytic and numerical models were developed to predict distortions in welded plates and shells. A simplified approach to this problem is the Inherent strain method, initially realized by Ueda et al. (1975). Several practical applications of this method are developed for thin and moderately thick plates (Murakawa et al. (2012); Lu et al. (2019); Ma et al. (2016)).

Residual stress can influence fatigue life, facilitating, inter alia, crack formation (see, for example, Hensel et al. (2018)) that is dangerous when combined with the embrittlement of material. However, it is obvious that compressive residual stress could increase the fatigue strength. There are several hammer peening techniques to generate these compression stresses and very local plastic deformation on the seam zone (Lefebvre et al. (2015)). In equipment working at high temperature, creep resistance is worsened by the residual stress near the welded zones.

Post Weld Heat Treatment (PWHT) obtain good results in residual stress relaxation with an improvement of creep and fatigue life of the joint (Dong, Song, and Zhang (2014)). Unfortunately, in certain circumstances, the application of PWHT is not possible; for example, when the welded joint is too large to heat or situated in an inaccessible zone.

Weld residual stresses can be evaluated with codes, standards, and structural integrity assessment procedures like R6 procedure, API579 code, ASME codes, etc. In scientific literature, many works focus on the applications and critical verifications of these codes (Bouchard (2007); Brickstad and Josefson (1998)). Standards and codes are applicable to specific components and often have a conservative evaluation of the residual stresses.

Welding numerical simulations are still essential to predict residual stress in specific welded components in order to verify the effective stress state in operative conditions. Analysis results can help to decide whether post-weld treatments are necessary or not. Complete FE simulations of large welded equipment are challenging to achieve because of their high computational cost.

Usually, in strength assessments, simulations of large piping and vessels are numerically implemented by shell elements to avoid the above-mentioned high computational cost. For this reason, in this paper, it is proposed an innovative parametric FE model to simulate longitudinal butt weldings using shell elements. This method can be easily integrated into the usual numerical analyses for the structural strength assessments.

2. Model description

As touched upon previously, the new FE equivalent model developed can simulate longitudinal multi-pass welding of plates by thermal transient analysis and static structural analysis.

The equivalent model can be divided into two zones: the Multiconnected Zone (MZ), containing the heat altered zone (HAZ), centred on the weld centerline and the Outer Zone (OZ) that is the remaining zone.

The model is composed essentially by four-noded shell elements in both zones. The nodal plane is not centred in the middle of the thickness, but it is at the top or at the bottom. The multiconnected zone is obtained by superimposing N distinct shell elements. There are as many overlapped shell elements as the number of welding passes that compose the joint (Fig. 1).

The Outer zone is realised by N-layer shell elements. N represents the number of welding passes in this case, too. Every level in the MZ and every layer in the OZ has an assigned thickness that represents the height of the relevant welding pass.

In the equivalent model, the MZ was developed in order to evaluate rotations, translations and local stress state typical of a multi-passes weld during all the welding process.

In thermal and structural analysis, filler material deposition is simulated by deactivating the entire seam weld in the first step of the simulation. Elements are reactivated step by step to simulate the torch movement and material

deposition. The ratio between the longitudinal length of elements reactivated in a step and the step time determines the welding speed.

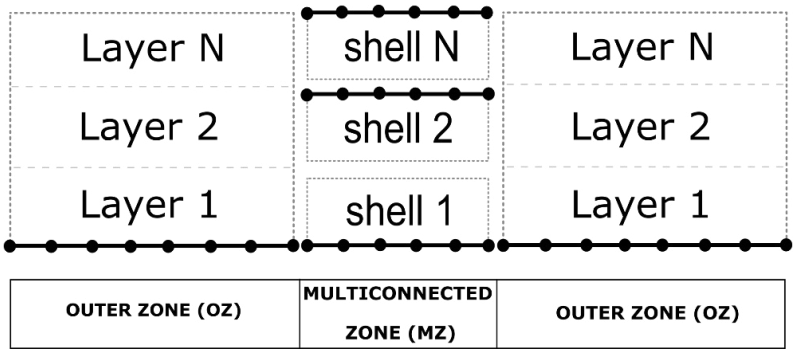

Fig. 1. Schematic representations of the FE equivalent model

2.1. Thermal model

During a process of welding, the movement of the torch causes extremely localised and significant temperature gradients that govern residual stress and distortion. In welding simulations, transient thermal analyses are necessary to predict temperature gradients inside and outside the HAZ during the whole time history of the welding.

In the thermal configuration, the equivalent model is provided with constraint equations to connect the thermal degrees of freedom of the various levels in the MZ. A parametric subroutine automatically generates constraint equations between the nodes of the overlapping levels, re-establishing the thermal conduction between them (Trupiano et al. (2019)).

Analogously, another subroutine is developed so that it thermally interconnects the Multiconnected Zone with the Outer Zone. Constraint equations connect the thermic nodal DOFs of the N levels composing the MZ with the thermic nodal DOFs of the N layers of the OZ (Trupiano et al. (2019)).

In the thermal configuration, the equivalent model is also equipped with two-noded thermal link elements. Link elements are generated automatically between the N levels of the MZ. Shell elements and link elements are thermally connected by constraint equations (Fig. 2).

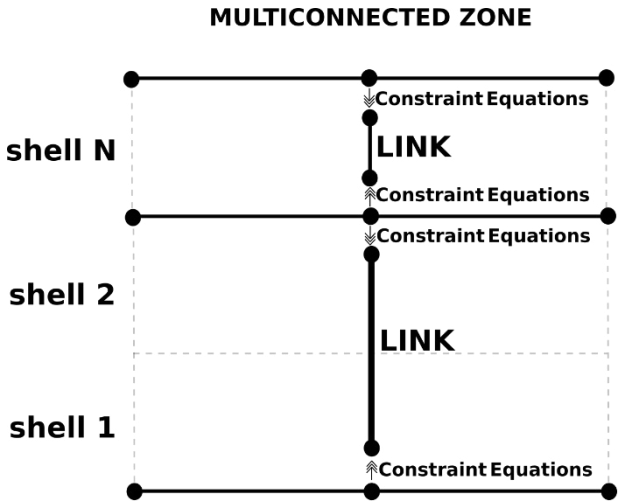

Fig. 2. Constraint equations between link and shell elements

It is not possible to directly merge thermal shell nodes and link nodes because the elements have different thermal DOFs.

Link elements are included in the thermal analysis only to store nodal temperature history for the subsequent structural analysis. These elements are defined with very low thermal conductivity, specific heat and density as not to alter thermal analysis results. The utility of link elements and relevant thermic DOFs will be explained in the next paragraph.

Thermal simulation of the welding process can be implemented by imposing a heat flux or by fixing the temperature of the melted bead. In scientific literature, there are several models of heat flux with different grade of accuracy (Goldak and Akhlaghi (2005); Lindgren (2007)). In the thermal analysis, the proposed model can operate with constant plane heat flux and Gaussian plane heat flux or by imposing a temperature to the elements in the fused zone.

2.2. Structural model

The equivalent structural model is carried out by the equivalent thermal model with a subroutine that changes thermal elements into structural elements; thermal constraint equations are deleted. Thermal shell elements are switched into structural shell ones, while the thermal link elements are transformed into two-noded 3D RIGID beam elements. In the structural configuration, the beam elements are connected between the nodes of the N levels of the MZ (Fig. 3). Rigid elements also permit the mechanical connection between the MZ and the OZ.

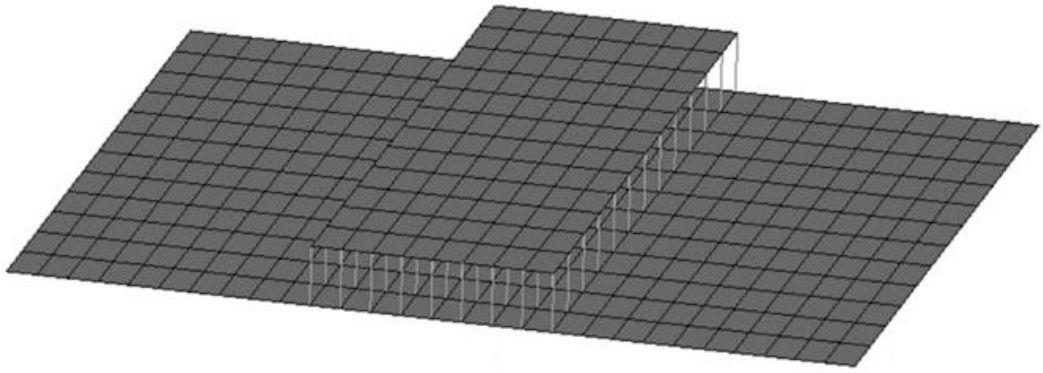

Fig. 3. Structural configuration of the equivalent model

Beam and shell elements are automatically connected by three translation constraint equations and three rotation constraint equations for each node. Direct merging of nodes is not possible as not to lose thermal DOFs that are different in the two types of elements. Rigid beams allow to re-establish kinematic congruence between shell elements. In the MZ, the rigid connection between levels is in accordance with Kirchhoff-Love's theory. Initially, beam elements are normal to the shell levels and remain straight after deformation.

Temperature history (that is the result of thermal analysis) is imported in structural analysis. The thermal DOFs of two-nodes link elements are transferred to two-nodes rigid beam elements. In this way, the equivalent model can replicate the thermal expansion in the thickness direction, which is essential to reproduce a more accurate kinematics of the joint during the welding simulation**.**

3. FE analysis

In this chapter, an application of the proposed model is reported. A FEA of a longitudinal welding of a steel plate is performed. Complete transient thermal analysis and elastoplastic analysis are realized to simulate a two-pass square groove welding.

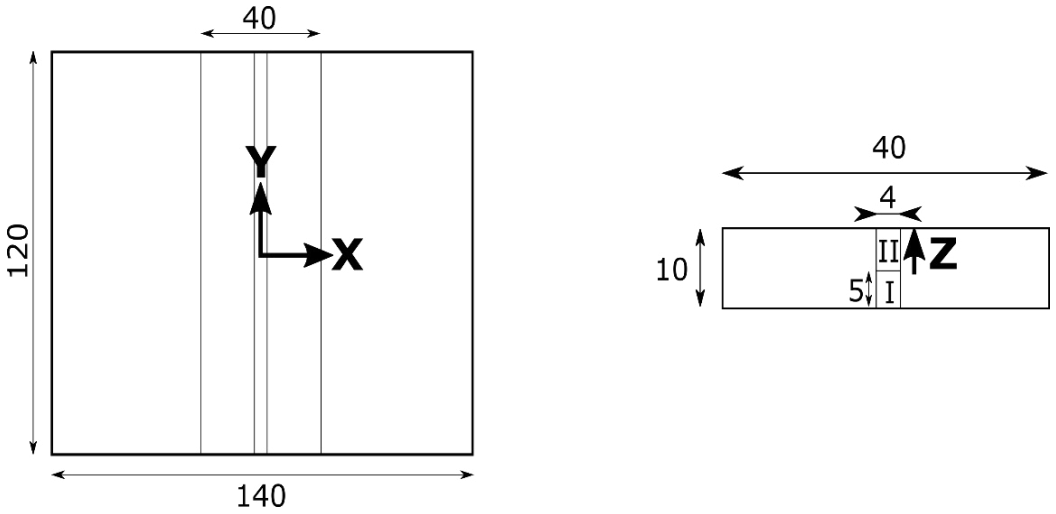

Fig. 4. a) Plate geometry,sizes are in mm; b) Multiconnected zone detail, sizes are in mm

The plate geometry and the coordinate system used to illustrate the results are shown in Fig. 4a. A section view of the MZ, with in detail the geometry of the passes, is displayed in Fig. 4b.

In order to verify the proposed model, a 3D solid model is used as a benchmark to thermal and structural results. The solid model is composed of 11520 elements and 13689 nodes, with six elements per pass along the thickness. The equivalent shell model is composed of 1266 elements, 1651 nodes and about 3200 thermal or structural constraint equations. As a result, the thermal-structural FE simulations of the welded plates, with the proposed model, are several times faster than the simulations realized with brick elements.

3.1. Thermal Analysis

In all the time history of the welding simulation, the temperature distribution is obtained by a transient analysis. In this paper, phenomena like material phase changing and the radiation heat loss have been neglected, taking into account only heat exchange by conduction and convection. An imposed temperature of 1500 °C is applied to the seam elements that are reactivated step by step during the analysis. In this way, the movement and the heat flux supplied by a welding torch are simulated. The chosen welding speed is 10 mm/s. The thermal properties of the steel plate are plotted in Fig. 5. At “liquidus” temperature, thermal conductivity should be more than doubled to consider a higher convection heat exchange of the molten steel (Song and Dong (2016)).

The results of the thermal analysis of the solid and the new equivalent shell models are shown in Fig. 6a and b. Near the centerline (CL) of the welding, the maximum difference of temperature between the two models is detected when the “torch” is in the proximity of the analyzed zone.

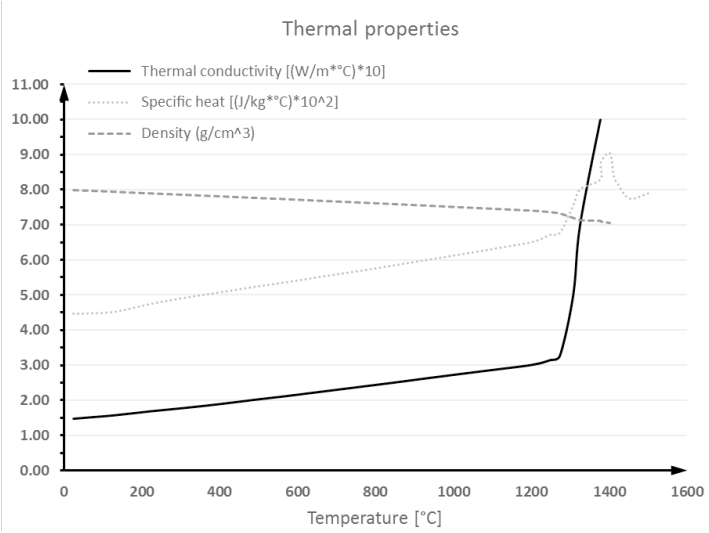

Fig. 5. Thermal properties of the steel utilized in the FE analysis

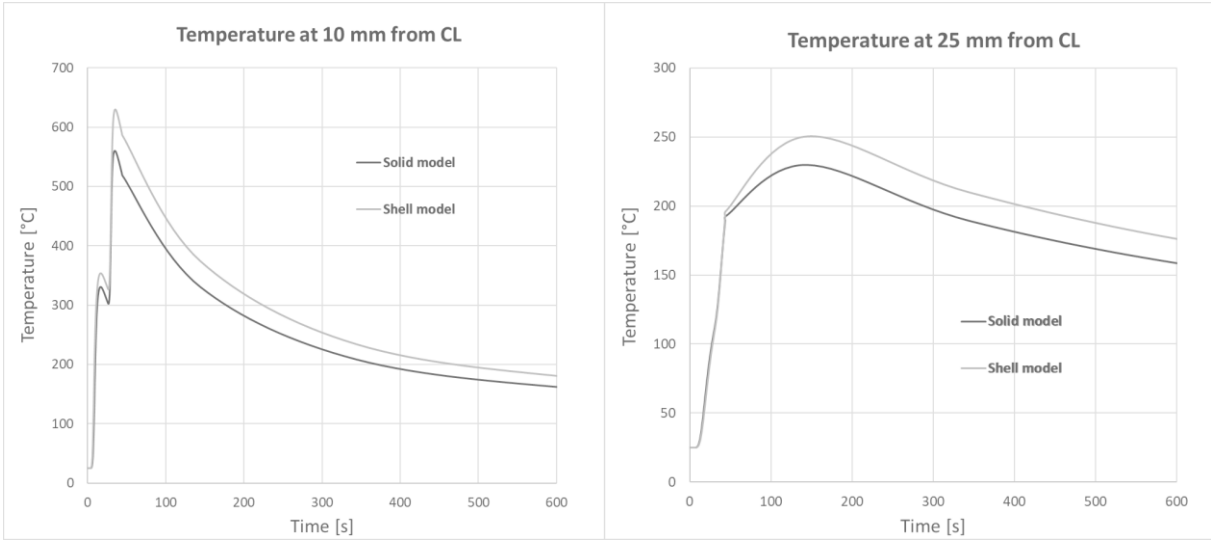

Fig. 6. a) Temperature in Y= 0 mm, X= 10 mm on top face (Z= 5 mm); b) Temperature in Y= 0 mm, X= 25 mm on bottom face (Z = -5mm)

3.2. Structural analysis

The structural elastoplastic analyses are developed with a rate-independent plasticity. A cut off temperature is assumed at 1200 °C. Cut off temperature is the value above which elastoplastic properties do not change (Goldak and Akhlaghi (2005); Lindgren (2007)). The mechanical properties of the material are reported in Fig. 7 and in Table 1.

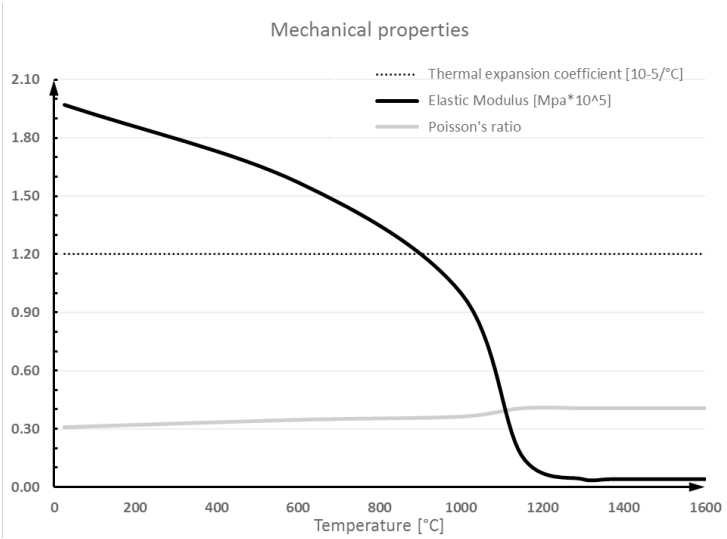

Fig. 7. Mechanical properties of the steel utilized in the FE analysis

Table 1. Other Mechanical properties of the steel utilized in the FE analysis

Temperature [°C]	Yield Strength [MPa]	Tensile Strength [MPa]
25	320	620
600	124	380
1000	100	300

As regards the boundary conditions of the FE models, the plate is fixed on the length side, see Fig. 8. The A, B, C path lines to which the results refer are further reported in Fig. 8.

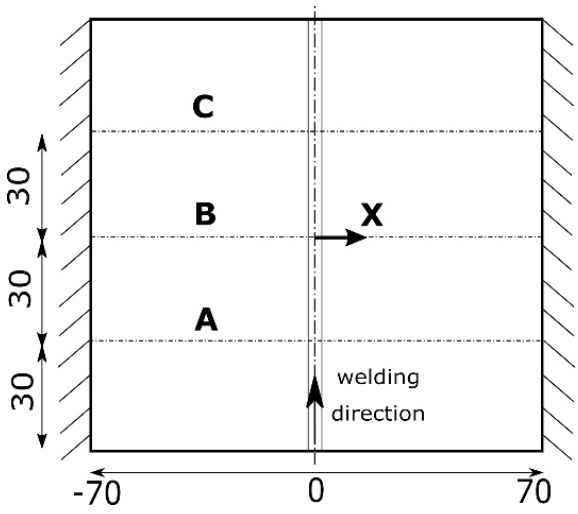

Fig. 8. Plate constraint conditions and path lines of the results, size are in mm.

The resulting residual stresses of the FE simulation, after the complete cooldown of the plate, are reported below. All the results are reported neglecting the seam zone because of the very low mechanical property of melted metal in the weld pool defined in the modelling. The residual stresses observed on the top surface of the three paths are shown from the Fig. 9 to the Fig. 11. The same stresses, measured at different depth along the thickness at mid-thickness and on the bottom surface for conciseness only at the path B, are plotted from the Fig. 12 and Fig. 13.

Residual stress data of the proposed equivalent model are in excellent agreement with solid model results.

In particular, the main trend of stresses is well simulated by the equivalent model whatever is the patch reported. Nearby the constraint the stress values present localized deviations. This is due to the impossibility of shell elements in the OZ to consider the z-axis expansion, completely constrained in the solid model. In a component application of the procedure, this error influence is negligible because no constraints are so close to the seam as in this validation case.

Dissimilarities in residual stresses and distortions between the two models are also present near the weld toe and the weld root. The 3D model, with six elements per pass along the thickness, could take into account more accurately the extremely local phenomenon in these zones. In addition, the outlines of the groove reach melting temperature when the welding torch is in proximity. The considerations given for the seam zone still apply in this case as well.

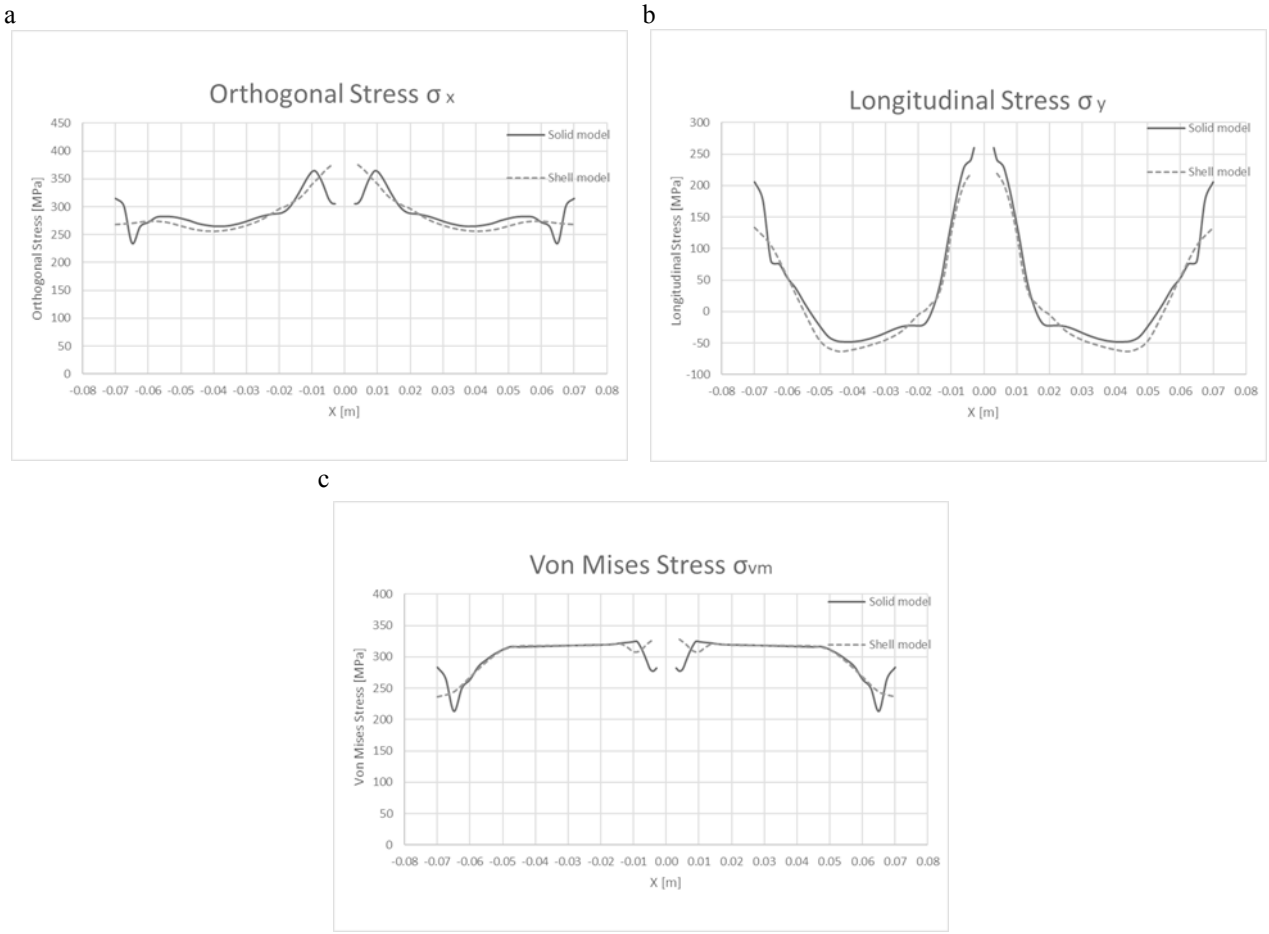

Fig. 9. Orthogonal stress (a), longitudinal stress (b) and Von Mises stress (c) on top surface path A (end of cooldown)

a

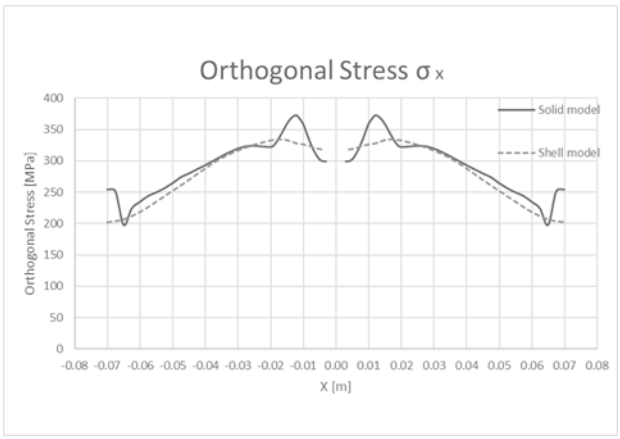

b

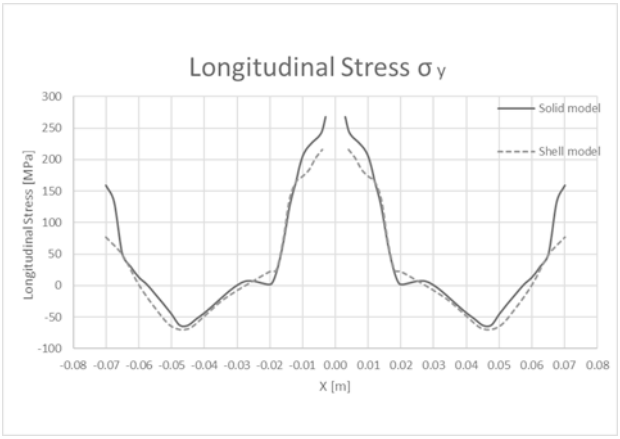

c

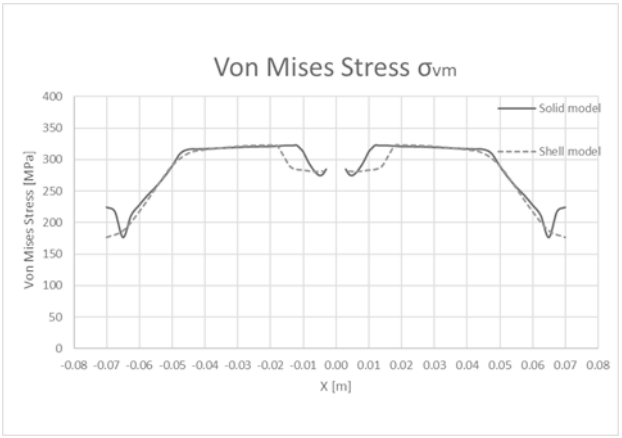

Fig. 10. Orthogonal stress (a), longitudinal stress (b) and Von Mises stress (c) on top surface path B (end of cooldown)

a

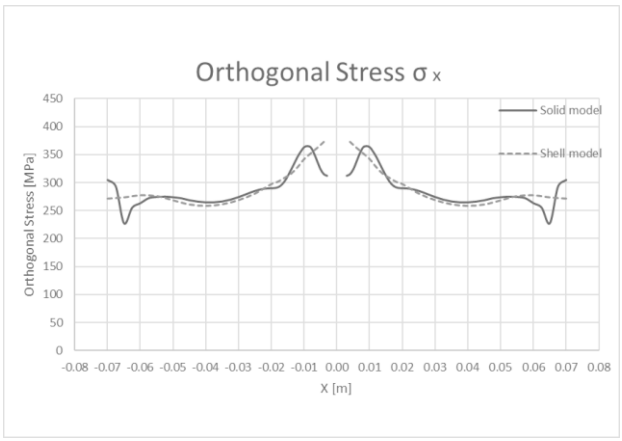

b

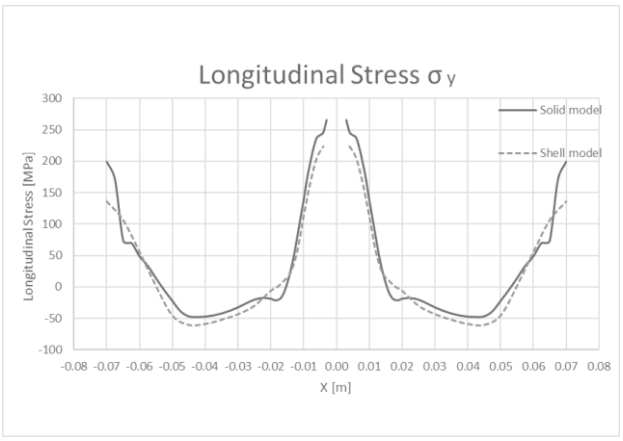

c

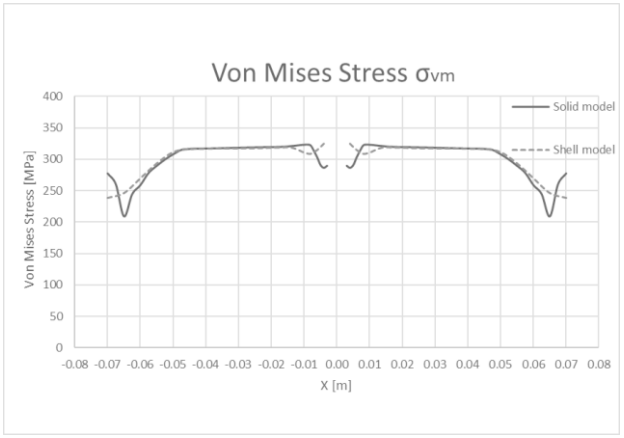

Fig. 11. Orthogonal stress (a), longitudinal stress (b) and Von Mises stress (c) on top surface path C (end of cooldown)

a

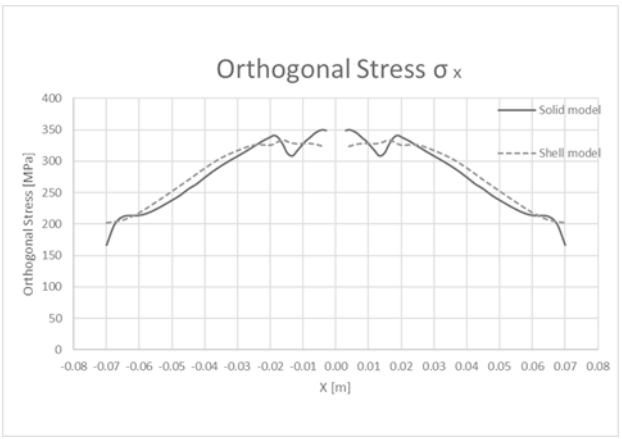

b

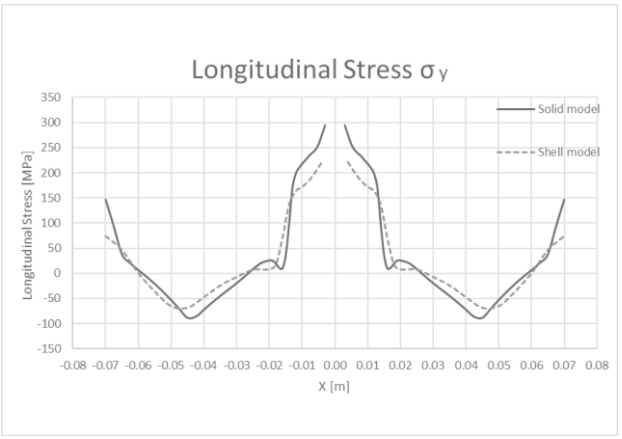

c

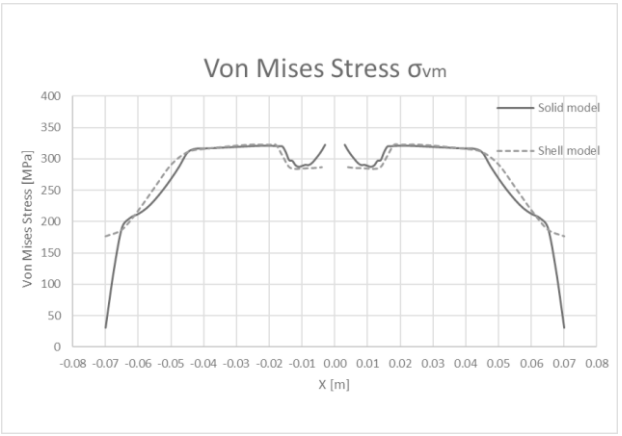

Fig. 12. Orthogonal stress (a), longitudinal stress (b) and Von Mises stress (c) at mid-thickness path B (end of cooldown)

Distortions of the plate on A path, at the complete cooldown, are shown in Fig. 14. The distortion of the two models are in good agreement too.

Especially in x direction the displacements are very well simulated, while a bigger error is present in y direction even if these displacements are sensibly smaller than in x direction.

To demonstrate the proper working of the model during the welding process, the residual stresses and distortions observed at the end of the first pass deposition are reported from the Fig. 15 and Fig. 16.

Even in this case, the stresses and distortions are comparable with good accuracy.

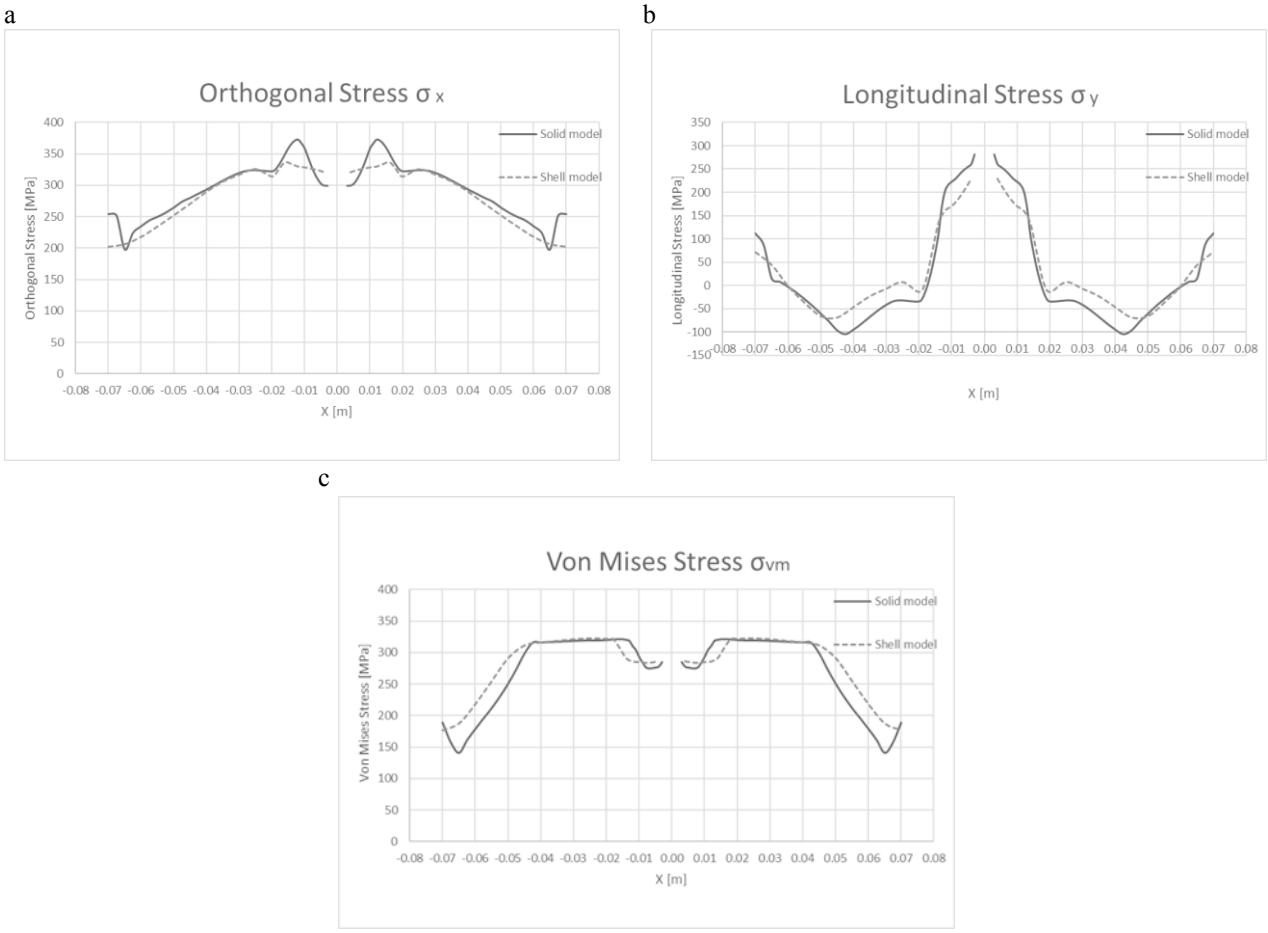

Fig. 13. Orthogonal stress (a), longitudinal stress (b) and Von Mises stress (c) on bottom surface path B (end of cooldown)

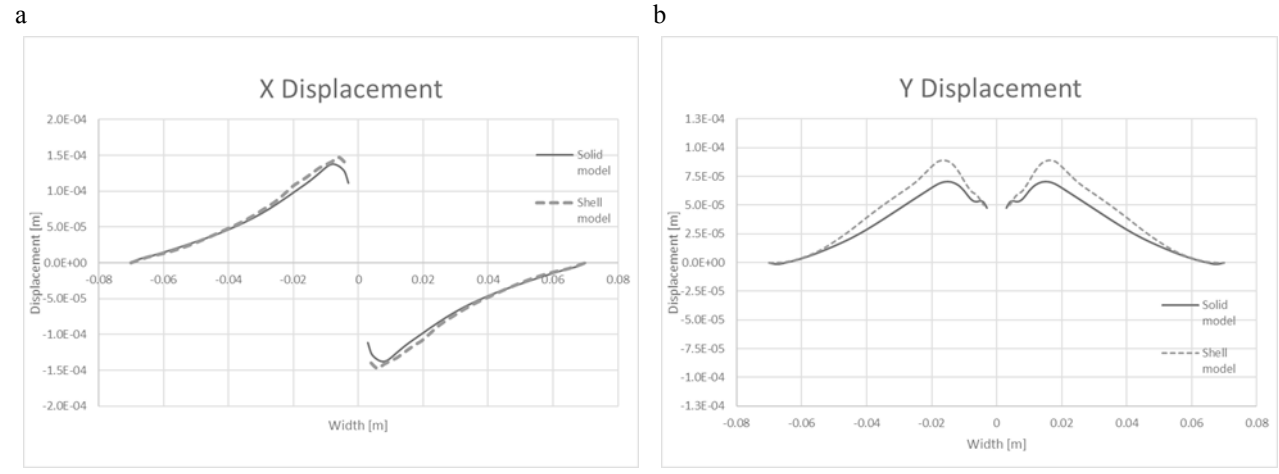

Fig. 14. X-displacement (a) and Y-displacement (b) on path A (end of cooldown)

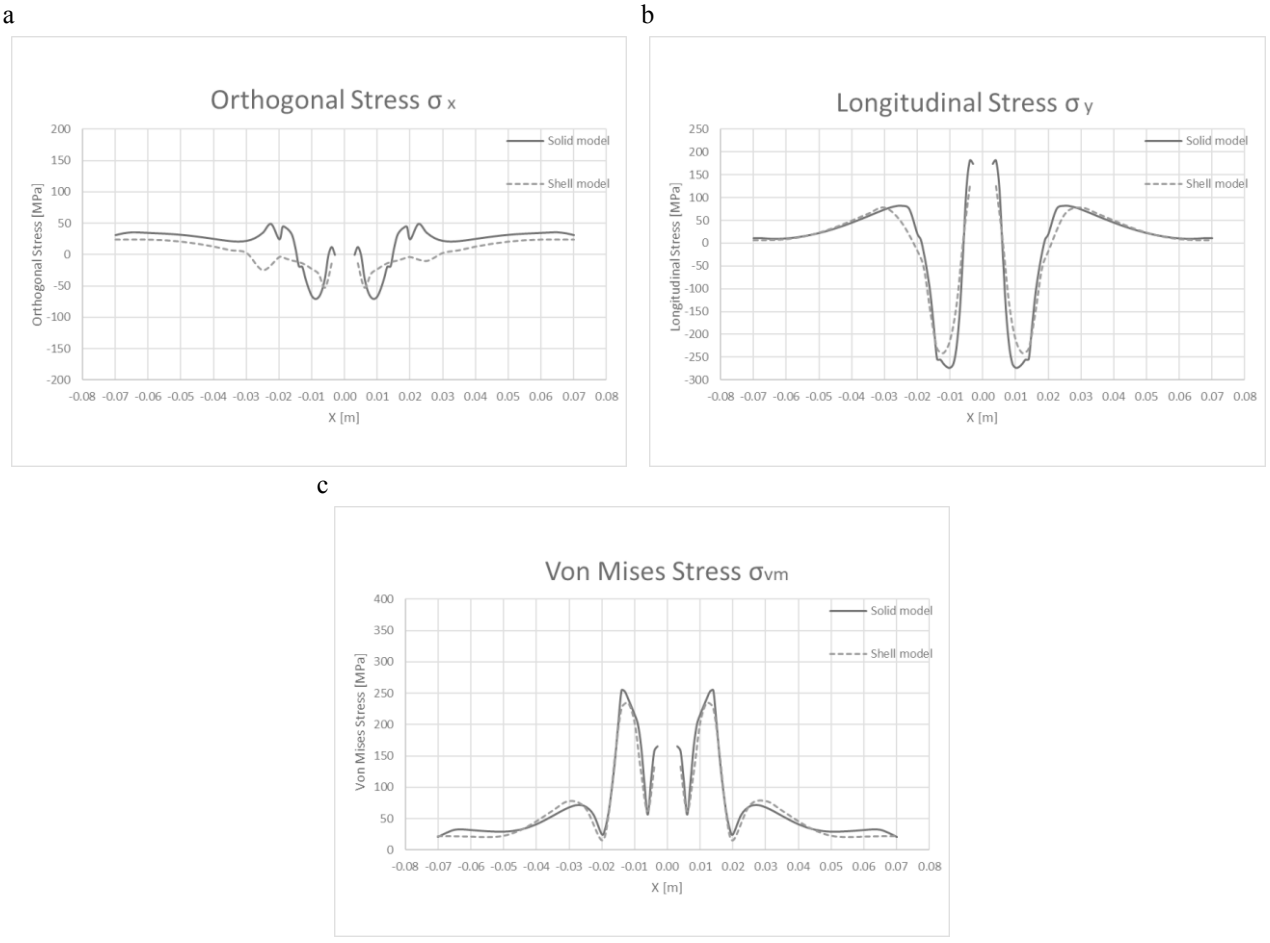

Fig. 15. Orthogonal stress (a), longitudinal stress (b) and Von Mises stress (c) at mid-thickness path B (end of the first pass)

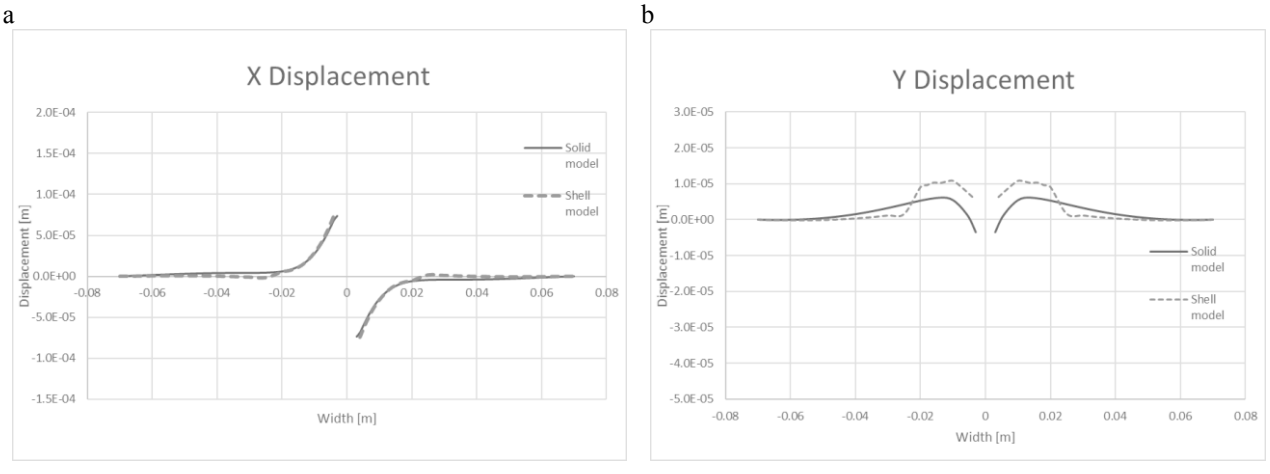

Fig. 16. X-displacement (a) and Y-displacement (b) on path B (end of the first pass)

4. Conclusions

In conclusion, an innovative FE model was developed to simulate multi-pass welding of plates. This model can be used almost automatically in pre-existent geometries by means of its total parameterization. Thanks to the use of four-noded shell elements, two-noded beam elements and constraint equations, the proposed model guarantees low computational costs and allows to simulate large welded joints in less time than a simulation with solid elements. To demonstrate the effectiveness of the model mentioned above, this one was applied to simulate a two-passes longitudinal butt welding process. A complete thermal-structural analysis is achieved with a rate-independent elastoplastic material. Residual stresses and distortion obtained during and after the simulated welding process are in good agreement with the results of the solid FE model made of height-noded brick elements.

5. References

Bouchard, P.J. 2007. "Validated Residual Stress Profiles for Fracture Assessments of Stainless Steel Pipe Girth Welds." International Journal of Pressure Vessels and Piping 84 (4): 195–222. https://doi.org/10.1016/j.ijpvp.2006.10.006.

Brickstad, B., and B. L. Josefson. 1998. "A Parametric Study of Residual Stresses in Multi-Pass Butt-Welded Stainless Steel Pipes." International Journal of Pressure Vessels and Piping 75 (1): 11–25. https://doi.org/10.1016/S0308-0161(97)00117-8.

Dong, Pingsha, Shaopin Song, and Jinmiao Zhang. 2014. "Analysis of Residual Stress Relief Mechanisms in Post-Weld Heat Treatment." International Journal of Pressure Vessels and Piping 122 (1): 6–14. https://doi.org/10.1016/j.ijpvp.2014.06.002.

Goldak, John A., and Mehdi Akhlaghi. 2005. Computational Welding Mechanics. Boston: Kluwer Academic Publishers. https://doi.org/10.1007/b101137.

Hensel, J., T. Nitschke-Pagel, D. Tchoffo Ngoula, H. Th Beier, D. Tchuindjang, and U. Zerbst. 2018. "Welding Residual Stresses as Needed for the Prediction of Fatigue Crack Propagation and Fatigue Strength." Engineering Fracture Mechanics 198: 123–41. https://doi.org/10.1016/j.engfracmech.2017.10.024.

Lefebvre, Fabien, Catherine Peyrac, Guillaume Elbel, C. Revilla-Gomez, Catherine Verdu, and Jean Yves Buffière. 2015. "Understanding of Fatigue Strength Improvement of Steel Structures by Hammer Peening Treatment." Procedia Engineering 133: 454–64. https://doi.org/10.1016/j.proeng.2015.12.615.

Lindgren, Lars-Erik. 2007. Computational Welding Mechanics. 1st ed. Woodhead Publishing.

Lu, Yaohui, Chuan Lu, Dewen Zhang, Tianli Chen, Jing Zeng, and Pingbo Wu. 2019. "Numerical Computation Methods of Welding Deformation and Their Application in Bogie Frame for High-Speed Trains." Journal of Manufacturing Processes 38 (September 2018): 204–13. https://doi.org/10.1016/j.jmapro.2019.01.013.

Ma, Ninshu, Keiji Nakacho, Takahiko Ohta, Naoki Ogawa, Akira Maekawa, Hui Huang, and Hidekazu Murakawa. 2016. "Inherent Strain Method for Residual Stress Measurement and Welding Distortion Prediction." In Volume 9: Prof. Norman Jones Honoring Symposium on Impact Engineering; Prof. Yukio Ueda Honoring Symposium on Idealized Nonlinear Mechanics for Welding and Strength of Structures, V009T13A001. ASME. https://doi.org/10.1115/OMAE2016-54184.

Murakawa, Hidekazu, Dean Deng, Ninshu Ma, and Jiangchao Wang. 2012. "Applications of Inherent Strain and Interface Element to Simulation of Welding Deformation in Thin Plate Structures." Computational Materials Science 51 (1): 43–52. https://doi.org/10.1016/j.commatsci.2011.06.040.

Song, Shaopin, and Pingsha Dong. 2016. "A Framework for Estimating Residual Stress Profile in Seam Welded Pipe and Vessel Components Part II: Outside of Weld Region." International Journal of Pressure Vessels and Piping 146: 65–73. https://doi.org/10.1016/j.ijpvp.2016.07.010.

Trupiano, S., Belardi, G.V., Fanelli, P., Vivio, F., Gaetani, L. 2019. "A novel approach to model multi-passes seam welding of butt joints.", Under review.

Ueda, Yukio, Keiji Fukuda, Keiji Nakacho, and Setsuo Endo. 1975. "A New Measuring Method of Residual Stresses with the Aid of Finite Element Method and Reliability of Estimated Values." Journal of the Society of Naval Architects of Japan 1975 (138): 499–507. https://doi.org/10.2534/jjasnaoe1968.1975.138_499.